Prostate-specific membrane antigen radioguided surgery to detect nodal metastases in primary prostate cancer patients undergoing robot-assisted radical prostatectomy and extended pelvic lymph node dissection: results of a planned interim analysis of a prospective phase 2 study

Gandaglia, G.; Mazzone, E.; Stabile, A.; Pellegrino, A.; Cucchiara, V.; Barletta, F.; ... ; Briganti, A.

Surgery in Motion

Prostate-specific membrane antigen Radioguided Surgery to Detect Nodal Metastases in Primary Prostate Cancer Patients Undergoing Robot-assisted Radical Prostatectomy and Extended Pelvic Lymph Node Dissection: Results of a Planned Interim Analysis of a Prospective Phase 2 Study

Giorgio Gandaglia [a,b,*], *Elio Mazzone* [a,b], *Armando Stabile* [a,b], *Antony Pellegrino* [a,b], *Vito Cucchiara* [a,b], *Francesco Barletta* [a,b], *Simone Scuderi* [a,b], *Daniele Robesti* [a,b], *Riccardo Leni* [a,b], *Ana Maria Samanes Gajate* [c], *Maria Picchio* [b,c], *Luigi Gianolli* [c], *Giorgio Brembilla* [b,d], *Francesco De Cobelli* [b,d], *Matthias N. van Oosterom* [e], *Fijs W.B. van Leeuwen* [e], *Francesco Montorsi* [a,b], *Alberto Briganti* [a,b]

[a] *Unit of Urology/Division of Oncology, Gianfranco Soldera Prostate Cancer Lab, IRCCS IRCCS San Raffaele Scientific Institute, Milan, Italy;* [b] *Vita-Salute San Raffaele University, Milan, Italy;* [c] *Nuclear Medicine Department, IRCCS San Raffaele Scientific Institute, Milan, Italy;* [d] *Department of Radiology, IRCCS San Raffaele Scientific Institute, Milan, Italy;* [e] *Interventional Molecular Imaging Laboratory, Department of Radiology, Leiden University Medical Centre, Leiden, The Netherlands*

Article info

Abstract

Background: Extended pelvic nodal dissection (ePLND) represents the gold standard for nodal staging in prostate cancer (PCa). Prostate-specific membrane antigen (PSMA) radioguided surgery (RGS) could identify lymph node invasion (LNI) during robot-assisted radical prostatectomy (RARP).
Objective: To report the planned interim analyses of a phase 2 prospective study (NCT04832958) aimed at describing PSMA-RGS during RARP.
Design, setting, and participants: A phase 2 trial aimed at enrolling 100 patients with intermediate- or high-risk cN0cM0 PCa at conventional imaging with a risk of LNI of >5% was conducted. Overall, 18 patients were enrolled between June 2021 and March 2022. Among them, 12 patients underwent PSMA-RGS and represented the study cohort.
Surgical procedure: All patients received ^{68}Ga-PSMA positron emission tomography (PET)/magnetic resonance imaging; ^{99m}Tc-PSMA-I&S was synthesised and administered intravenously the day before surgery, followed by single-photon emission computed tomography/computed tomography. A Drop-In gamma probe was used for in vivo

* Corresponding author. Unit of Urology/Division of Oncology, URI, IRCCS Ospedale San Raffaele, Milan, Italy. Tel. +39 02.2643.4066; Fax: +39 02.2643.7286.
E-mail address: Gandaglia.giorgio@hsr.it (G. Gandaglia).

measurements. All positive lesions (count rate ≥2 compared with background) were excised and ePLND was performed.

Measurements: Side effects, perioperative outcomes, and performance characteristics of robot-assisted PSMA-RGS for LNI were measured.

Results and limitations: Overall, four (33%), six (50%), and two (17%) patients had intermediate-risk, high-risk, and locally advanced PCa. Overall, two (17%) patients had pathologic nodal uptake at PSMA PET. The median operative time, blood loss, and length of stay were 230 min, 100 ml, and 5 d, respectively. No adverse events and intraoperative complications were recorded. One patient experienced a 30-d complication (Clavien-Dindo 2; 8.3%). Overall, three (25%) patients had LNI at ePLND. At per-region analyses on 96 nodal areas, sensitivity, specificity, positive predictive value, and negative predictive value of PSMA-RGS were 63%, 99%, 83%, and 96%, respectively. On a per-patient level, sensitivity, specificity, positive predictive value, and negative predictive values of PSMA-RGS were 67%, 100%, 100%, and 90%, respectively.

Conclusions: Robot-assisted PSMA-RGS in primary staging is a safe and feasible procedure characterised by acceptable specificity but suboptimal sensitivity, missing micrometastatic nodal disease.

Patient summary: Prostate-specific membrane antigen radioguided robot-assisted surgery is a safe and feasible procedure for the intraoperative identification of nodal metastases in cN0cM0 prostate cancer patients undergoing robot-assisted radical prostatectomy with extended pelvic lymph node dissection. However, this approach might still miss micrometastatic nodal dissemination.

1. Introduction

Approximately one out of five contemporary prostate cancer (PCa) patients undergoing robot-assisted radical prostatectomy (RARP) with extended pelvic lymph node dissection (ePLND) harbour lymph node invasion (LNI) at final pathology [1]. Correct nodal staging plays a key role in the identification of pN1 patients who are typically characterised by a poor prognosis and could benefit from adjuvant therapies [1]. An ePLND aimed at removing all positive nodes might maximise local disease control and could theoretically have an impact on oncologic outcomes [2–4].

The sensitivity of conventional radiologic imaging (namely, computed tomography [CT] or magnetic resonance imaging [MRI]) for LNI is <40% even in the high-risk setting [5]. Although novel molecular imaging modalities such as prostate-specific membrane antigen (PSMA) positron emission tomography (PET) depicted higher accuracy than CT or MRI [5], these are still characterised by suboptimal performance characteristics in nodal staging, where their sensitivity does not exceed 60% [6]. Therefore, ePLND in patients at an increased risk of LNI still represents the most optimal method for nodal staging [7,8]. Available models to identify men at a higher risk of LNI based on clinical and biopsy parameters have excellent discrimination and calibration [8,9]. However, >65% of patients who are deemed as candidates for ePLND would eventually harbour negative lymph nodes at final pathology [9]. This overtreatment is particularly worrisome due to the prolonged operative time and the risk of complications associated with ePLND [10].

Recent studies have shown that radioactive labelling of PSMA ligands with gamma-emitting radionuclides such as 99m-technetium (eg, ^{99m}Tc-PSMA-I&S) can be used to per-

form PSMA-based radioguided surgery (PSMA-RGS) [11–13]. This approach, theoretically, could facilitate the identification of nodal metastases during surgery and allow for the identification of micrometastatic disease that would be missed by preoperative conventional and molecular imaging due to their intrinsic spatial resolution [11–13]. Multiple studies reported the safety, feasibility, and oncologic results of PSMA-RGS in patients with oligorecurrent PCa receiving open surgery after curative-intent therapies [11,13–15]. The evidence, however, is much scarcer regarding the role of this approach in the primary setting to identify LNI and/or for the robot-assisted technique feasibility [12,16,17].

The current study describes the planned interim analyses of a phase 2 prospective trial aimed at assessing the safety, feasibility, and accuracy of robot-assisted PSMA-RGS for the identification of LNI in PCa patients without evidence of nodal or distant metastases at conventional imaging who are candidates for RARP with concomitant ePLND. The current report aims at describing the technique and surgical safety of robot-assisted PSMA-RGS in this setting after completion of the study procedures in the first 12 cases.

2. Patients and methods

2.1. Study design

This is the planned analysis of a phase 2, single-institution, national, noncomparative, nonrandomised, prospective study (NCT04832958) started in November 2020, which is currently enrolling PCa patients with no evidence of nodal or distant metastases (cN0cM0) at conventional imaging who are candidates for RARP with ePLND and have a risk of LNI >5% according to the Briganti nomogram [18]. The main exclusion criteria are represented by the receipt of neoadjuvant therapies, previous

PCa treatments, or inclusion in other experimental trials. The full study protocol as well as the eligibility criteria are provided in the Supplementary material. This prospective trial will enrol a total of 100 PCa patients and was funded through a competitive grant by the Italian Ministry of Health (Giovani Ricercatori GR2018-12368369). The current preplanned analysis aims at reporting the safety and feasibility of [99mTc]-PSMA-RGS after the first ten cases (18-mo milestone). Owing to a higher-than-expected enrolment rate, a total of 18 patients have been screened between June 2021 and March 2022. Among them, 12 patients underwent [99mTc]-PSMA-RGS with available pathologic and 30-d follow-up information, and represented the study cohort.

2.2. Evaluation with [68Ga]-PSMA PET/MRI and [99mTc]-PSMA SPECT/CT

At least 1 wk before surgery, all patients underwent [68Ga]-PSMA PET/MRI scan (median activity: 149 MBq) for preoperative staging, as previously described (Fig. 1) [19]. All PSMA PET scans were evaluated by dedicated experienced nuclear medicine physicians (A.M.S.G. and M.P.). The results of preoperative [68Ga]-PSMA PET/MRI did not change the initially planned treatment. After approval of the Italian Medicines Agency, [99mTc]-PSMA-I&S was prepared using a synthesis kit (piCHEM, Raaba-Grambach, Austria) and administered the day before RARP and ePLND (20 h before surgery; median activity: 735 MBq) [20]. SPECT/CT imaging was performed after 270 min from the administration of [99mTc]-PSMA-I&S to document tracer uptake, and it served as a quality control. Positive [68Ga]-PSMA PET/MRI and [99mTc]-PSMA-I&S PET/CT were defined as the presence of any uptake at the level of the pelvic and/or retroperitoneal nodes.

2.3. Surgical technique

All procedures were performed through a transperitoneal approach using the Da Vinci Xi (Intuitive Surgical, Sunnyvale, CA, USA) robotic surgical system by two experienced surgeons using a standardised technique (A.B. and G.G.). After incision of the peritoneum, release of the bladder laterally to the endopelvic fascia and identification of the ureters, a sterilisable, commercially available, CE-marked Drop-In gamma probe (Crystal Drop-In Probe; Crystal Photonics, Berlin, Germany) inserted through a 15-mm assistant port placed above the right iliac crest was used for in vivo intraoperative measurements to identify metastatic lesions in the internal iliac, external iliac, obturatory, and common iliac stations. Intraoperative measurements with the Drop-In gamma probe were performed at the common iliac (above ureteric crossing), presacral, and retroperitoneal stations. The Crystal Drop-In Probe has been specifically designed for the application in robotic surgery. The probe, which has a 10-mm head, can be inserted through a 12 or 15 mm assistant trocar, and can be autonomously grasped and directed by the console surgeon using robotic ProGrasp forceps [15]. A control unit provides both acoustic and numerical feedback as a response to [99mTc] activity and can be used for intraoperative surgical guidance. A positive finding was defined as the presence of a count rate of at least twice that of the background reference (namely, the homolateral fatty tissue of each patient). All positive lesions (a count rate of at least twice that of the background reference) were excised [11]. Ex vivo gamma measurements were performed to confirm the removal of the radioactive lesion or to prompt further search in case of a missing signal. All the removed tissue was collected separately according to the anatomical site of resection. Anatomically defined ePLND was then performed, which included the fibrofatty tissue along the external iliac vein, the lateral limit being the genitofemoral nerve and the distal limit being the deep circumflex vein [8]. Proximally, the cranial limit was represented by the crossing between the ureter and common iliac vessels. All fibrofatty tissue within the obturator fossa was removed. The dissection was performed from lateral to medial up to the umbilical artery, and the bladder wall represented the medial limit. Lymph nodes along, as well as medially and laterally to, the internal iliac vessels were removed. The RARP was then completed according to a previously described technique [21].

2.4. Outcomes and follow-up

Perioperative outcomes, which included operative time, blood loss, length of stay, and intraoperative and 30-d postoperative complications, were prospectively collected according to the European Association of Urology (EAU) Guidelines Panel recommendations on reporting and grading complications [22]. All tissue specimens removed during ePLND including regions positive at PSMA-RGS were evaluated by a dedicated

PSMA-RGS PROCEDURES

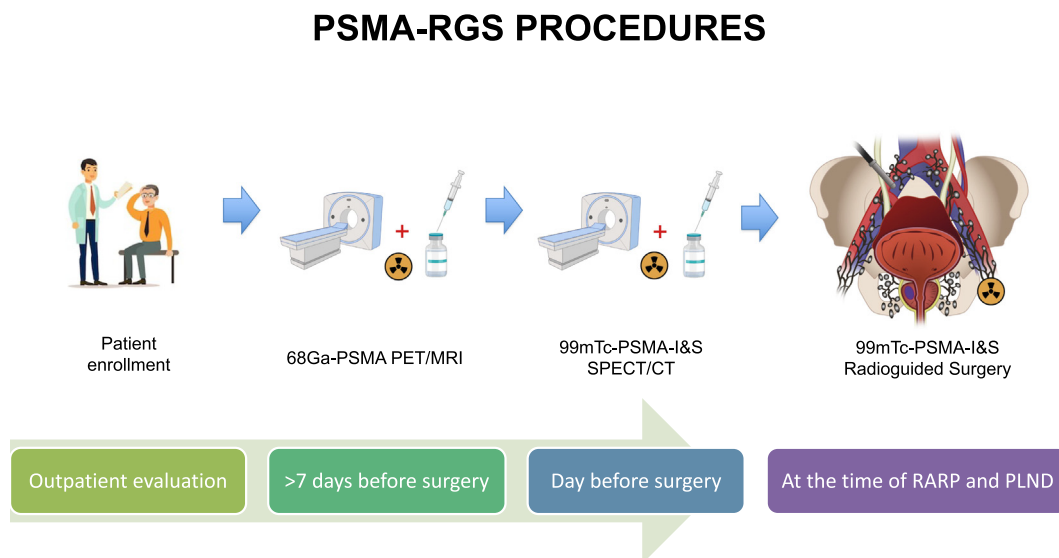| Patient enrollment	68Ga-PSMA PET/MRI	99mTc-PSMA-I&S SPECT/CT	99mTc-PSMA-I&S Radioguided Surgery
Outpatient evaluation	>7 days before surgery	Day before surgery	At the time of RARP and PLND

Fig. 1 – Study procedures: PSMA-RGS. CT = computed tomography; MRI = magnetic resonance imaging; PET = positron emission tomography; PLND = pelvic nodal dissection; PSMA = prostate-specific membrane antigen; RARP = robot-assisted radical prostatectomy; RGS = radioguided surgery; SPECT = single-photon emission computed tomography.

pathologist. The pathologic evaluation represented the gold standard to assess the predictive characteristics of PSMA-RGS for the identification of LNI, which was defined as the presence of positive lymph nodes at final pathology. The first serum prostate-specific antigen (PSA) measurement was performed at 6 wk after surgery, and PSA persistence was defined as a PSA value of >0.1 ng/ml. All patients included in the final cohort received the scheduled follow-up visits at 28 d after surgery according to the protocol.

2.5. Sample size calculation and statistical analyses

Owing to the innovative nature of our study and the lack of data on the performance characteristics of ^{99m}Tc-PSMA-RGS in nodal staging in the primary setting at the time of study design, we were not able to compute a formal sample size calculation. A total sample size of 100 consecutive patients will be enrolled in our study based on an empirical and feasibility approach. The current study reports the planned interim analysis after the first ten cases to describe the safety and feasibility of the technique in the primary staging setting, as per the study protocol. Medians and proportions were reported for continuous and categorical variables, respectively. Contingency tables were used to calculate the sensitivity, specificity, and positive (PPV) and negative (NPV) predictive values of PSMA-RGS compared with final pathology, which represented the gold standard, in per-patient and per-region analyses. All statistical analyses were performed using SPSS (version 22; IBM Statistics).

3. Results

3.1. Baseline characteristics

Table 1 depicts the characteristics of patients included in these interim analyses. The median age and PSA at surgery were 70 yr and 8.7 ng/ml, respectively. Overall, four (33%), six (50%), and two (17%) patients had EAU intermediate-risk, high-risk, and locally advanced disease, respectively. Biopsy grade groups were 2, 3, 4, and 5 in one (8.3%), five (52%), four (33%), and two (17%) patients, respectively. The median risk of LNI according to the Briganti nomogram was 17%. Overall, two (17%) patients had pathologic nodal uptake at ^{68}Ga-PSMA PET/MRI (median number of positive spots: 2).

3.2. Evaluation with ^{99m}Tc-PSMA SPECT/CT

No adverse events were recorded after the administration of ^{99m}Tc-PSMA-I&S. The SPECT/CT performed the day before surgery accurately identified the two (17%) patients with positive spots at ^{68}Ga-PSMA PET/MRI. However, it missed one region out of 11 (9%) identified at ^{68}Ga-PSMA PET/MRI (Table 2).

3.3. Surgical safety and perioperative outcomes

The median operative time and blood loss were 230 min and 100 ml, respectively (Table 3). No intraoperative complications were recorded during RARP with ePLND and PSMA-RGS. One patient experienced a respiratory 30-d complication (pneumonia) treated with antibiotic therapy (Clavien-Dindo 2), which was unlikely to be related to PSMA-RGS. The median length of hospital stay was 5 d.

3.4. Concordance between ^{68}Ga-PSMA PET/MRI, ^{99m}Tc-PSMA-RGS, and final pathology

The imaging modality ^{68}Ga-PSMA PET/MRI identified 11 positive spots in two patients and missed three positive regions at final pathology (Table 2). When considering the pelvic lymph nodes, the sensitivity, specificity, NPV, and PPV of ^{68}Ga-PSMA PET/MRI for pathologic nodal metastases were, respectively, 66%, 100%, 90%, and 100% at a per-patient analysis.

PSMA-RGS did not identify any additional suspicious area in the pelvic nodal region that was not previously iden-

Table 1 – Patient demographics and clinical characteristics at diagnosis

Characteristic	n = 12
Age (yr), median (IQR)	70 (66–71)
BMI (kg/m^2), median (IQR)	25 (23–26)
CCI (age adjusted), n (%)	
≤2	5 (42)
>2	7 (58)
PSA at biopsy (ng/ml), median (IQR)	8.7 (4.8–15.5)
PSA density (MRI; ng/ml/ml), median (IQR)	0.26 (0.16–0.46)
Clinical stage, n (%)	
cT1	3 (25)
cT2	6 (50)
>cT2	3 (25)
Prostate biopsy approach, n (%)	
Systematic	7 (58)
MRI targeted + systematic	5 (42)
Prostate biopsy cores, median (IQR)	
Number of overall cores	15 (13–15)
Number of positive cores	9 (7–11)
Number of systematic cores	12 (12–14)
Number of positive systematic cores	7 (6–10)
Number of MRI targeted cores	3 (3–3)
Number of positive MRI targeted cores	3 (1–3)
Biopsy grade group, n (%)	
2 (3 + 4)	1 (8.3)
3 (4 + 3)	5 (42)
4 (4 + 4)	4 (33)
5 (4 + 5 or 5 + 4)	2 (17)
EAU risk group, n (%)	
Localised, intermediate risk	4 (33)
Localised, high risk	6 (50)
Locally advanced	2 (17)
Risk of LNI according to the Briganti nomogram (median, IQR)	17 (6.7–76)
^{68}Ga-PSMA PET/MRI, no. of positive patients (%)	
Activity (MBq), median (IQR)	149 (126–196)
Prostate	12 (100)
Pelvic lymph nodes	2 (17)
Obturator	2 (17)
External iliac	2 (17)
Internal iliac	2 (17)
Common iliac	1 (8.3)
Median number of positive nodes	2
^{99m}Tc-PSMA SPECT, no. of positive patients (%)	
Activity (MBq), median (IQR)	735 (731–738)
Prostate	11 (92)
Pelvic lymph nodes	2 (17)
Obturator	1 (8.3)
External iliac	2 (17)
Internal iliac	2 (17)
Common iliac	1 (8.3)

BMI = body mass index; CCI = Charlson Comorbidity Index; EAU = European Association of Urology; IQR = interquartile range; LNI = lymph node invasion; MRI = multiparametric resonance imaging; PET = positron emission tomography; PSA = prostate-specific antigen; PSMA = prostate-specific membrane antigen; SPECT = single-photon emission computed tomography.

tified by ^{68}Ga-PSMA PET/MRI, with a 75% concordance rate. Detailed gamma probe findings with histopathologic correlation in the in vivo and ex vivo settings are included in Table 2. A total of 96 pelvic nodal specimens were resected, which included 256 lymph nodes (median 22 per patient, interquartile range 18–23). Overall, eight of the 96 resected pelvic nodal regions (8%) and 12 of the 256 pelvic lymph nodes had LNI at final pathology. Histopathology positive specimens had median in vivo and ex vivo counts of 53 (41–63) and 44 (27–58), respectively, while negative specimens showed median in vivo and ex vivo counts of 13 (10–19) and 2 (1–3), respectively (both $p = 0.001$).

The Drop-In probe detected suspicious nodes in five locations at in vivo evaluation. Of these, four contained PCa while one contained no cancer. The Drop-In probe did not detect increased uptake in 91 locations, of which 87 contained no cancer and four harboured LNI. The sensitivity, specificity, PPV, and NPV of PSMA-RGS at a per-region analysis were 50%, 99%, 80%, and 96%, respectively (Table 4). When combining in vivo and ex vivo evaluations, which used a different threshold for positivity and limited background noise, a superior accuracy was observed, where the sensitivity, specificity, PPV, and NPV of PSMA-RGS at a per-region analysis were 63%, 99%, 83%, and 96%, respectively (Table 5). On a per-patient level analysis, the Drop-In gamma probe for PSMA-RGS correctly identified two out of three patients with pN1 disease in the pelvic lymph nodes, and depicted sensitivity, specificity, PPV, and NPV of, respectively, 67%, 100%, 100%, and 90% (Table 6). While the two patients with LNI detected at PSMA-RGS had massive nodal invasion with extracapsular extension, the patient with false negative findings both at preoperative imaging and at PSMA-RGS had a maximum LNI diameter of 3 mm. Finally, two patients had LNI outside the ePLND template (perivesical nodes), which was not detected at

^{68}Ga-PSMA PET/MRI, ^{99m}Tc-PSMA SPECT/CT, and PSMA-RGS. Among those, one had LNI exclusively in the perivesical nodes. The presence of LNI in perivesical nodes was not considered a false negative of PSMA-RGS both in per-patient

Table 3 – Perioperative surgical and oncological characteristics

Characteristic	n = 12
Perioperative outcomes	
Operative time (min), median (IQR)	230 (213–259)
Blood loss (ml), median (IQR)	100 (100–100)
Intraoperative complications, n (%)	0 (0)
30-d complications, Clavien-Dindo 3, n (%)	1 (8.3)
Length of stay, median (IQR)	5 (4–5)
Pathological Gleason grade group, n (%)	
3 (4 + 3)	4 (33.3)
4 (4 + 4)	2 (16.7)
5 (4 + 5, 5 + 4, or 5 + 5)	6 (50)
Pathological stage, n (%)	
T3a	8 (66.7)
T3b	4 (33.3)
Dominant cancer side	
Right prostate	4 (33.3)
Left prostate	4 (33.3)
Bilateral	4 (33.3)
Positive surgical margins, n (%)	2 (16.7)
Variant histology, n (%)	
Cribriform	12 (100)
Intraductal	2 (17)
Ductal	2 (17)
Mucinous	2 (17)
Glomeruloid	1 (8.3)
Neuroendocrine	1 (8.3)
Nodal staging, n (%)	
pN1	4 (33)
Patients with positive nodes in the ePLND template	3 (25)
Number of nodes removed, median (IQR)	22 (19–23)
Number of positive nodes in pN1 patients, median (range)	3 (3–7)

ePLND = extended pelvic lymph node dissection; IQR = interquartile range.

Table 2 – Preoperative ^{68}Ga-PSMA PET/MRI, ^{99m}Tc-PSMA SPECT/CT, and intraoperative PSMA-RGS results (in vivo and ex vivo evaluation) compared with final histopathologic evaluation in 12 patients treated with RARP and ePLND

	^{68}Ga-PSMA PET/MRI	^{99m}Tc PSMA SPECT/CT	PSMA RGS	Pathology results (number of positive nodes)
Patient 1	OR	OR	IIR	OL (1)
	EIR	EIR	IIL	EIR (1)
	IIR	IIR	OL	IIR (3)
	CIR	OL		IIL (2)
	OL	EIL		
	EIL	IIL		
	IIL	CIL		
	CIL			
Patient 2	Negative	Negative	Negative	PV (1)
Patient 3	Negative	Negative	Negative	Negative
Patient 4	OL	OL	EIL	IIL (1)
	EIL	EIL	OL	OL (1)
	IIL	IIL		EIL (1)
Patient 5	Negative	Negative	Negative	Negative
Patient 6	Negative	Negative	Negative	Negative
Patient 7	Negative	Negative	Negative	Negative
Patient 8	Negative	Negative	Negative	Negative
Patient 9	Negative	Negative	Negative	Negative
Patient 10	Negative	Negative	Negative	Negative
Patient 11	Negative	Negative	Negative	Negative
Patient 12	Negative	Negative	Negative	OR (2; maximum diameter: 3 mm) PV (1)

CIL = common iliac left; CIR = common iliac right; CT = computed tomography; EIL = external iliac left; EIR = external iliac right; ePLND = extended pelvic lymph node dissection; IIL = internal iliac left; IIR = internal iliac right; MRI = multiparametric resonance imaging; OL = obturator left; OR = obturator right; PET = positron emission tomography; PSMA = prostate-specific membrane antigen; PV = perivesical; RARP = robot-assisted radical prostatectomy; RGS = radioguided surgery; SPECT = single-photon emission computed tomography.

Table 4 – Contingency table and diagnostic accuracy on per-region analysis over a total of 96 anatomical lymph nodal regions dissected (RGS positivity defined as a count of at least twice that of the background at in vivo evaluation only)

	Pathology positive	Pathology negative
PSMA RGS positive	4	1
PSMA RGS negative	4	87
Sensitivity	50%	
Specificity	99%	
Positive predictive value	80%	
Negative predictive value	96%	

PSMA = prostate-specific membrane antigen; RGS = radioguided surgery.

Table 5 – Contingency table and diagnostic accuracy on per-region analysis over a total of 96 pelvic anatomical lymph nodal regions dissected (RGS positivity defined as a count of at least twice that of the background at in vivo or ex vivo evaluation)

	Pathology positive	Pathology negative
PSMA RGS positive	5	1
PSMA RGS negative	3	87
Sensitivity	63%	
Specificity	99%	
Positive predictive value	83%	
Negative predictive value	96%	

PSMA = prostate-specific membrane antigen; RGS = radioguided surgery.

Table 6 – Contingency table and diagnostic accuracy on per-patient analysis (RGS positivity defined as a count of at least twice that of the background at in vivo or ex vivo evaluation)

	Pathology positive	Pathology negative
PSMA RGS positive	2	0
PSMA RGS negative	1	9
Sensitivity	67%	
Specificity	100%	
Positive predictive value	100%	
Negative predictive value	90%	

PSMA = prostate-specific membrane antigen; RGS = radioguided surgery.

and per-region analyses for two reasons: (1) the perivesical area is outside the ePLND template and (2) the performance characteristics of PSMA-based imaging in the perivesical area are suboptimal due to the high background noise.

3.5. Follow-up

No side effects associated with the administration of ^{99m}Tc-PSMA-I&S and with the use of the CE-marked, commercially available, Drop-In Crystal gamma probe were reported at the first follow-up visit at 28 d. Overall, three (25%) patients had PSA persistence after RARP. Of note, two patients had pN1 disease with massive nodal invasion at final pathology, and one patient had LNI in the perivesical nodes. All patients with PSA persistence were candidates for salvage radiotherapy after multidisciplinary evaluation.

4. Discussion

Previous studies suggested a role for PSMA-RGS in the detection of LNI in patients with positive PSMA PET/CT undergoing salvage lymph node dissection [11,13,14,20].

However, evidence is scarce regarding the feasibility of this approach in both primary setting and robot-assisted surgery [12]. In the face of such a paucity of data, we planned to describe the surgical technique and report the safety and feasibility of robot-assisted PSMA-RGS after having performed the first ten out of 100 cases in a prospective phase 2 trial that is currently enrolling cN0cM0 patients at conventional imaging with intermediate- and high-risk PCa who are candidates for RARP with ePLND. These analyses were originally planned in the trial protocol. Owing to the higher-than-expected enrolment rate, we can report the results of the first 12 patients who completed the study procedures.

Our results are several-fold. First, the effective synthesis and distribution of ^{99m}Tc-PSMA-I&S, which was synthesised using previously described methodologies [20], have been documented in virtually all patients included by SPECT/CT performed 270 min after tracer injection. Moreover, the administration of ^{99m}Tc-PSMA-I&S was safe, where no side effects were recorded. Similarly, robot-assisted PSMA-RGS using a CE-marked Drop-In gamma probe, which was controlled by the robotic arms, was a feasible and safe procedure; no intra- or postoperative complications related to this technique were recorded, and only a minor impact on the operative time was observed [22]. Taken together, these observations suggest that PSMA-RGS can be performed during RARP with ePLND without additional risks for the patient.

Second, although our findings should be considered preliminary and the assessment of the performance characteristics of PSMA-RGS is beyond the scope of this interim analysis, the use of the Drop-In gamma probe to detect ^{99m}Tc uptake intraoperatively depicted acceptable specificity at both per-region and per-patient analyses with sensitivity that was not optimal. Indeed, PSMA-RGS correctly identified two patients as pN1. Both men had nodal uptake at preoperative ^{68}Ga-PSMA PET/MRI. However, PSMA-RGS, as well as PSMA PET/MRI, failed to detect obturatory right positive nodes in a patient who had a micrometastatic nodal involvement (maximum diameter: 3 mm) exclusively in this region. This resulted in per-patient sensitivity, specificity, PPV, and NPV of, respectively, 67%, 100%, 100%, and 90%. Although the combination of both in vivo and ex vivo measurements was able to identify most regions with LNI at final pathology, PSMA-RGS depicted sensitivity slightly higher than 60% also at a per-region analysis with specificity and PPV ≥96%. PSMA-RGS failed to identify two regions with LNI at final pathology in patients correctly staged as pN1 (n = 2). However, the laterality of PSMA-RGS was concordant with preoperative PET and final pathology in both cases. Of note, both patients with pN1 disease and uptake at PSMA-RGS had more than two positive nodes with massive nodal involvement and extranodal extension [23]. This suggests that the risk of underestimation associated with the use of PSMA PET before surgery in patients with a high nodal burden might also apply to PSMA-RGS [24]. We hypothesised that the use of PSMA-RGS might overcome the limits related to the spatial resolution of preoperative PSMA imaging and allow for the detection of micrometastatic lymph nodes that would otherwise be

missed by PET scans [11]. However, this technique missed a case of micrometastatic LNI that was not detected by preoperative imaging in one patient. Taken together, these findings suggest that for the time being, PSMA-RGS is still characterised by suboptimal sensitivity. On the contrary, the specificity of this technique, both in vivo and ex vivo, should be used to confirm the removal of suspicious nodes at preoperative PSMA PET. Indeed, negative findings at PSMA-RGS should guide the surgeon towards more extended dissection in men with positive spots at preoperative PSMA PET, to identify nodal metastases even outside the standard template [12].

Gondoputro et al. [12] recently reported the results of 12 PCa patients undergoing ⁹⁹ᵐTc-PSMA-I&S RGS in the primary setting, and observed higher sensitivity at a per-region analysis with lower specificity and PPV than our findings. These discrepancies should be considered in the context of the dissimilarities between the two trials. First, a different threshold for PSMA-RGS positivity was adopted (1.5 vs 2 times the background reference). Of note, the performance characteristics of PSMA-RGS improved substantially in both trials when considering ex vivo measurements, which limit the effect of the background noise and should therefore be considered a crucial part of the procedure. Second, while our study focused on intermediate- and high-risk patients, Gondoputro et al. [12] included a population of high-risk PCa. This resulted in substantially higher preoperative PSMA PET positivity (64% vs 17%) and LNI (83% vs 33%). This underscores the critical role that patient selection plays in PSMA-targeted surgery. Third, while we used a CE-marked Drop-In gamma probe, they tested a prototype.

From a clinical standpoint, our study represents one of the first reports describing the safety and feasibility of robot-assisted PSMA-RGS in the primary staging setting in intermediate- and high-risk PCa patients. Moreover, our study is the first report describing the use of a CE-marked Drop-In gamma probe that is sterilisable and that maintained its performance quality in these first 12 patients. The Drop-In gamma probe can be grasped easily and manipulated by the console surgeon during RARP, providing immediate intraoperative feedbacks on the removal of nodal metastases at the time of surgery. Our preliminary results suggest that PSMA-RGS is safe and is not associated with an increased risk of adverse perioperative outcomes. No intra- or postoperative complications that can directly be referred to PSMA-RGS have been reported. The Drop-In gamma probe assisted surgeons in the intraoperative detection of PSMA-avid lesions, and no technical difficulties were reported. The longer length of hospital stay than what was reported in patients who underwent RARP without PSMA-RGS [25] might be related to different reasons. First, hospital admission occurred the day before surgery for tracer injection. Second, the inclusion of the first patients receiving this surgical procedure might have resulted in a more prudential behaviour when considering hospital discharge, to allow for the prompt recognition and management of side effects. Finally, all patients included in our cohort underwent ePLND, which is typically associated with a longer length of stay compared to pNx patients [26]. Despite this, our findings suggest that PSMA-RGS can facilitate the identification of LNI particularly in patients with nodal uptake at preoperative PSMA PET. At the time being, the main benefits associated with PSMA-RGS reside in the immediate intraoperative feedback on the removal of all PSMA-avid tissue identified by preoperative PET or SPECT imaging. The lack of an increased count rate detected by the Drop-In gamma probe in the resected tissue should result in more extended nodal dissection aimed at identifying nodal metastases that would have otherwise been missed. This is particularly true when PSMA-positive spots are located outside the ePLND template area or in anatomical regions that are difficult to dissect at the time of RARP. Nonetheless, the PSMA-RGS technique was associated with an underestimation of the real nodal burden at final pathology even in men with pN1 disease correctly detected by the Drop-In probe. As such, PSMA-RGS cannot be used to omit ePLND when indicated according to preoperative characteristics, and an anatomically defined ePLND should be performed even when an uptake is detected by the Drop-In probe.

Despite the prospective nature of our study and the use of standardised procedures in all patients enrolled, some limitations should be considered. First, we report the outcomes of the first 12 patients undergoing PSMA-RGS; a total of 100 men will be enrolled. As such, our results should be considered preliminary. In this context, we cannot exclude that a learning-curve phenomenon applies to this surgical approach and, therefore, that the predictive characteristics of robot-assisted PSMA-RGS might improve over time once the technique has been refined. Second, we report short-term data, and a longer follow-up is needed to assess stronger endpoints. Finally, our results were obtained at a high-volume tertiary referral centre with extensive experience in robot-assisted surgery and nuclear medicine, and therefore, might not be generalisable to other settings.

5. Conclusions

Robot-assisted ⁹⁹ᵐTc-PSMA-RGS is a safe and feasible procedure that could allow for the intraoperative identification of nodal metastases in cN0cM0 PCa patients undergoing RARP with ePLND. However, although PSMA-RGS might assist surgeons in the identification of LNI during ePLND, our preliminary data suggest that the sensitivity of this procedure might not be adequate for the detection of micrometastatic nodal dissemination.

Peer Review Summary

Peer Review Summary and Supplementary data to this article can be found online at https://doi.org/10.1016/j.eururo.2022.06.002.

References

[1] Marra G, Valerio M, Heidegger I, et al. Management of patients with node-positive prostate cancer at radical prostatectomy and pelvic lymph node dissection: a systematic review. Eur Urol Oncol 2020;3:565–81.

[2] Abdollah F, Gandaglia G, Suardi N, et al. More extensive pelvic lymph node dissection improves survival in patients with node-positive prostate cancer. Eur Urol 2015;67:212–9.

[3] Fossati N, Parker WP, Karnes RJ, et al. More extensive lymph node dissection at radical prostatectomy is associated with improved outcomes with salvage radiotherapy for rising prostate-specific antigen after surgery: a long-term, multi-institutional analysis. Eur Urol 2018;74:134–7.

[4] Lestingi JFP, Guglielmetti GB, Trinh QD, et al. Extended versus limited pelvic lymph node dissection during radical prostatectomy for intermediate- and high-risk prostate cancer: early oncological outcomes from a randomized phase 3 trial. Eur Urol 2021;79:595–604.

[5] Hofman MS, Lawrentschuk N, Francis RJ, et al. Prostate-specific membrane antigen PET-CT in patients with high-risk prostate cancer before curative-intent surgery or radiotherapy (proPSMA): a prospective, randomised, multicentre study. Lancet 2020;395:1208–16.

[6] Stabile A, Pellegrino A, Mazzone E, et al. Can negative prostate-specific membrane antigen positron emission tomography/computed tomography avoid the need for pelvic lymph node dissection in newly diagnosed prostate cancer patients? A systematic review and meta-analysis with backup histology as reference standard. Eur Urol Oncol 2022;5:1–17.

[7] Mottet N, van den Bergh RCN, Briers E, et al. EAU-EANM-ESTRO-ESUR-SIOG guidelines on prostate cancer—2020 update. Part 1: screening, diagnosis, and local treatment with curative intent. Eur Urol 2021;79:243–62.

[8] Gandaglia G, Ploussard G, Valerio M, et al. A novel nomogram to identify candidates for extended pelvic lymph node dissection among patients with clinically localized prostate cancer diagnosed with magnetic resonance imaging-targeted and systematic biopsies. Eur Urol 2019;75:506–14.

[9] Gandaglia G, Martini A, Ploussard G, et al. External validation of the 2019 Briganti nomogram for the identification of prostate cancer patients who should be considered for an extended pelvic lymph node dissection. Eur Urol 2020;78:138–42.

[10] Cacciamani GE, Maas M, Nassiri N, et al. Impact of pelvic lymph node dissection and its extent on perioperative morbidity in patients undergoing radical prostatectomy for prostate cancer: a comprehensive systematic review and meta-analysis. Eur Urol Oncol 2021;4:134–49.

[11] Maurer T, Robu S, Schottelius M, et al. ^{99m}Technetium-based prostate-specific membrane antigen–radioguided surgery in recurrent prostate cancer. Eur Urol 2019;75:659–66.

[12] Gondoputro W, Scheltema MJ, Blazevski A, et al. Robot-assisted prostate-specific membrane antigen-radioguided surgery in primary diagnosed prostate cancer. J Nucl Med. In press. https://doi.org/10.2967/jnumed.121.263743.

[13] Horn T, Krönke M, Rauscher I, et al. Single lesion on prostate-specific membrane antigen-ligand positron emission tomography and low prostate-specific antigen are prognostic factors for a favorable biochemical response to prostate-specific membrane antigen-targeted radioguided surgery in recurrent prostate cancer. Eur Urol 2019;76:517–23.

[14] Knipper S, Tilki D, Mansholt J, et al. Metastases-yield and prostate-specific antigen kinetics following salvage lymph node dissection for prostate cancer: a comparison between conventional surgical approach and prostate-specific membrane antigen-radioguided surgery. Eur Urol Focus 2019;5:50–3.

[15] de Barros HA, van Oosterom MN, Donswijk ML, et al. Robot-assisted prostate-specific membrane antigen-radioguided salvage surgery in recurrent prostate cancer using a DROP-IN gamma probe: the first prospective feasibility study. Eur Urol 2022;82:97–105.

[16] Taneja SS. Re: Darolutamide in nonmetastatic, castration-resistant prostate cancer. J Urol 2019;202:660–1.

[17] Van Leeuwen FWB, Van Oosterom MN, Meershoek P, et al. Minimal-invasive robot-assisted image-guided resection of prostate-specific membrane antigen-positive lymph nodes in recurrent prostate cancer. Clin Nucl Med 2019;44:580–1.

[18] Briganti A, Larcher A, Abdollah F, et al. Updated nomogram predicting lymph node invasion in patients with prostate cancer undergoing extended pelvic lymph node dissection: the essential importance of percentage of positive cores. Eur Urol 2012;61:480–7.

[19] Mapelli P, Ghezzo S, Samanes Gajate AM, et al. Preliminary results of an ongoing prospective clinical trial on the use of 68 Ga-PSMA and 68 Ga-DOTA-RM2 PET/MRI in staging of high-risk prostate cancer patients. Diagnostics (Basel, Switzerland) 2021;11:2068.

[20] Robu S, Schottelius M, Eiber M, et al. Preclinical evaluation and first patient application of 99mTc-PSMA-I&S for SPECT imaging and radioguided surgery in prostate cancer. J Nucl Med 2017;58:235–42.

[21] Martini A, Falagario UG, Villers A, et al. Contemporary techniques of prostate dissection for robot-assisted prostatectomy. Eur Urol 2020;78:583–91.

[22] Gandaglia G, Bravi CA, Dell'Oglio P, et al. The impact of implementation of the European Association of Urology Guidelines Panel recommendations on reporting and grading complications on perioperative outcomes after robot-assisted radical prostatectomy. Eur Urol 2018;74:4–7.

[23] Abdollah F, Jeffrey Karnes R, Suardi N, et al. Predicting survival of patients with node-positive prostate cancer following multimodal treatment. Eur Urol 2014;65:554–62.

[24] Fossati N, Scarcella S, Gandaglia G, et al. Underestimation of positron emission tomography/computerized tomography in assessing tumor burden in prostate cancer nodal recurrence: head-to-head comparison of 68 Ga-PSMA and 11 C-choline in a large, multi-institutional series of extended salvage lymph node dissections. J Urol 2020;204:296–301.

[25] Rosiello G, Gandaglia G, Scuderi S, et al. Reducing the risk of postoperative complications after robot-assisted radical prostatectomy in prostate cancer patients: results of an audit and feedback intervention following the implementation of prospective data collection. Eur Urol Focus 2022;8:431–7.

[26] Fossati N, Willemse PPM, Van den Broeck T, et al. The benefits and harms of different extents of lymph node dissection during radical prostatectomy for prostate cancer: a systematic review. Eur Urol 2017;72:84–109.